THE JOURNAL OF BIOLOGICAL CHEMISTRY VOL. 280, NO. 45, pp. 37877–37884, November 11, 2005

Molecular Basis for Zinc Potentiation at Strychnine-sensitive Glycine Receptors*

Received for publication, July 28, 2005 Published, JBC Papers in Press, September 6, 2005, DOI 10.1074/jbc.M508303200

Paul S. Miller[1], **Helena M. A. Da Silva, and Trevor G. Smart**[2]

From the Department of Pharmacology, University College London, Gower Street, London WC1E 6BT, United Kingdom

The divalent cation Zn^{2+} is a potent potentiator at the strychnine-sensitive glycine receptor (GlyR). This occurs at nanomolar concentrations, which are the predicted endogenous levels of extracellular neuronal Zn^{2+}. Using structural modeling and functional mutagenesis, we have identified the molecular basis for the elusive Zn^{2+} potentiation site on GlyRs and account for the differential sensitivity of GlyR α_1 and GlyR α_2 to Zn^{2+} potentiation. In addition, juxtaposed to this Zn^{2+} site, which is located externally on the N-terminal domain of the α subunit, another residue was identified in the nearby Cys loop, a region that is critical for receptor gating in all Cys loop ligand-gated ion channels. This residue acted as a key control element in the allosteric transduction pathway for Zn^{2+} potentiation, enabling either potentiation or overt inhibition of receptor activation depending upon the moiety resident at this location. Overall, we propose that Zn^{2+} binds to a site on the extracellular outer face of the GlyR α subunit and exerts its positive allosteric effect via an interaction with the Cys loop to increase the efficacy of glycine receptor gating.

The glycine receptor is a major component of inhibitory neurotransmission in the spinal cord and brainstem (1). It forms part of the Cys loop receptor family, which includes acetylcholine, γ-aminobutyric acid type A ($GABA_A$),[3] and serotonin type 3 receptors (2). Glycine receptors are pentameric assemblies of ligand binding $\alpha_{(1-4)}$ subunits and the homologous structural β subunit (3). Each subunit has an extracellular N-terminal domain followed by four transmembrane (TM) segments connected by two intracellular regions and an extracellular TM2-TM3 linker, which is important for receptor gating (4). The function of these receptors can be enhanced by a variety of agents, including alcohols, anesthetics, neurosteroids, and Zn^{2+} (5–8), but their exact binding sites and transduction pathways remain controversial.

However, Zn^{2+} binding sites do provide realistic targets for identification, as these are traditionally compact, consisting of only 3–4 residues, and their coordination chemistry is understood (9). With regard to GlyRs, Zn^{2+} exhibits biphasic activity, potentiating receptor activation at submicromolar Zn^{2+} concentrations and causing inhibition at concentrations >10 μM (8). A previous study demonstrates that the mutation D80A in the extracellular domain of the GlyR α_1 subunit ablated Zn^{2+} potentiation, and it is proposed that this residue participates in the direct coordination of Zn^{2+} (10, 11). However, an additional report indicates that the Zn^{2+} potentiation of responses to the partial agonist taurine, which binds to the same agonist site as glycine, is unaffected by mutating Asp-80. This suggests that either multiple Zn^{2+} binding sites exist or that this mutation induces an indirect allosteric effect on receptor function that selectively disrupts Zn^{2+} potentiation of responses to glycine rather than those to taurine (12). In accord with an indirect allosteric effect, mutations of several other residues in the TM2-TM3 linker are capable of disrupting Zn^{2+} potentiation, though none of these residues are chemically suitable for the direct coordination of Zn^{2+}.

The high sensitivity of the strychnine-sensitive GlyR to Zn^{2+} potentiation makes this receptor an ideal substrate for modulation by basal levels of Zn^{2+}. In a physiological context, Zn^{2+} is released following neuronal stimulation (13, 14) and can also modulate inhibitory neurotransmitter receptors at basal concentrations (15, 16). Furthermore, Zn^{2+} is concentrated into synaptic boutons that also contain either glutamate, GABA, or glycine in many areas of the brain, including the cortex, hippocampus, and spinal cord (17–19). Although the predicted concentration of Zn^{2+} resulting from presynaptic release is probably <10 μM (20), this is more than sufficient to modulate *N*-methyl-D-aspartate receptors, certain $GABA_A$ receptor subtypes, and GlyRs (8, 21). Indeed, low nanomolar basal Zn^{2+} concentrations are adequate to prolong the decay phase of glycinergic inhibitory postsynaptic currents (22).

In this study, we accounted for the differential sensitivity to Zn^{2+} potentiation of GlyR α_1 and GlyR α_2 by identifying the location of a single conserved residue in the N-terminal domain. Subsequently, by using structural homology modeling together with the identified residue underlying Zn^{2+} sensitivity, we established the molecular determinants for the elusive Zn^{2+} potentiation binding site. In doing so, we uncovered a prospective transduction residue for this site that is located in the Cys loop-gating domain, providing a plausible molecular pathway for Zn^{2+} potentiation of glycine receptor gating.

MATERIALS AND METHODS

cDNA Constructs—Human (h) wild-type cDNA constructs were used for hGlyR α_{1L}, hGlyR α_{2A}, and hGlyR β. Site-specific mutant cDNAs were prepared using the Stratagene Quikchange mutagenesis kit. The mutated sequences were confirmed by complete sequencing of the cDNA insert using an ABI sequencer.

Cell Culture and Transfection—Human embryonic kidney (HEK) cells (American Type Culture Collection CRL1573) were grown and transfected as previously documented (23). Plasmids of hGlyR cDNA clones were co-transfected in a ratio of 1:1 with enhanced green fluorescent protein (24). To co-express GlyR $\alpha\beta$ heteromers, β subunit cDNA was added in excess at a ratio of 20:1 to α subunit cDNA. HEK cells were plated onto poly-L-lysine-coated coverslips (100 μg/ml) sufficient to achieve 20% confluence and used for recording on the next day.

* This work was supported by the Medical Research Council and the Wellcome Trust. The costs of publication of this article were defrayed in part by the payment of page charges. This article must therefore be hereby marked "*advertisement*" in accordance with 18 U.S.C. Section 1734 solely to indicate this fact.

[1] A Wellcome Trust four year Ph.D. postgraduate student.

[2] To whom correspondence should be addressed: Dept. of Pharmacology, University College London, Gower St., London, WC1E 6BT, United Kingdom. Tel.: 0207-679-2013; Fax: 0207-679-7298; E-mail: t.smart@ucl.ac.uk.

[3] The abbreviations used are: $GABA_A$, γ-aminobutyric acid type A; $GABA_{A/C}R$, γ-aminobutyric acid receptor type A/C; GlyR, glycine receptor; HEK, human embryonic kidney; MTSEA, 2-aminoethyl-methanesulphonate; RI, reduced inhibition; TM, transmembrane.

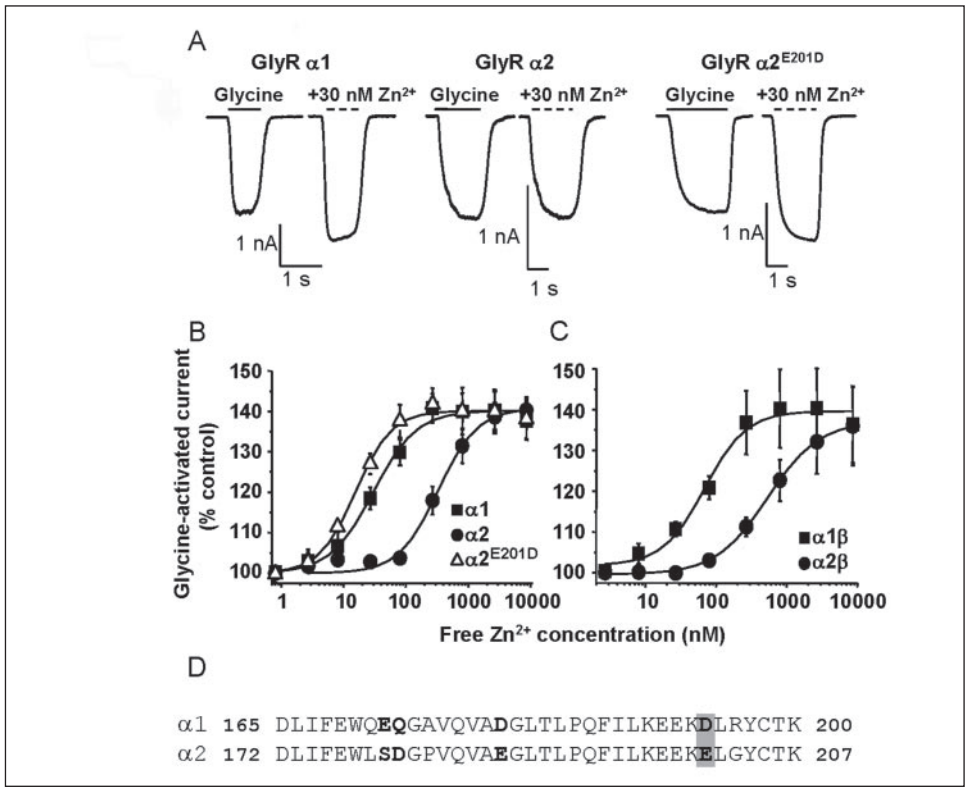

FIGURE 1. **Zn^{2+} potentiation of glycine-activated currents for GlyR α_1 and GlyR α_2.** Zn^{2+} concentration response curves were determined for the modulation of EC_{50} responses to glycine recorded in the presence of 10 mM tricine from HEK cells. *A*, typical glycine (EC_{50})-activated currents in the presence and absence of 30 μM Zn^{2+} for GlyR α_1, α_2, and α_2E201D. Zn^{2+} concentration curves for homomeric GlyR α_1, α_2, or α_2E201D (*B*) or heteromeric GlyR $\alpha_1\beta$ or $\alpha_2\beta$ (*C*) ($n = 4–6$). *D*, amino acid sequence alignment of GlyR α_1 and GlyR α_2 showing the region of the N-terminal extracellular domain that contains differences in potential Zn^{2+} binding residues (*bold*). A *gray filled box highlights* the residue responsible for the differential sensitivity to Zn^{2+}-mediated potentiation between GlyR α_1 and α_2. All numbering is for the mature protein.

Solutions—The internal pipette solution contained (mM): 140 KCl, 2 $MgCl_2$, 1 $CaCl_2$, 10 HEPES, 11 EGTA, and 2 ATP, pH 7.2 (≈ 300 mosM). The external Krebs solution consisted of (mM): 140 NaCl, 4.7 KCl, 1.2 $MgCl_2$, 2.5 $CaCl_2$, 10 HEPES, and 11 D-glucose, pH 7.4 (≈ 300 mosM). For those experiments requiring control over the basal levels of Zn^{2+} (see Fig. 1), tricine was used with an assumed K_D for Zn^{2+} complexation of 10^{-5} M (25). Thus, 0.26, 0.78, 2.6, 7.8, 26, 77.5, 254, and 775 μM Zn^{2+} provided effective free Zn^{2+} concentrations of 0.8, 2.68, 8, 26.8, 80, 268, 2680, and 8620 nM, respectively (calculated with WINMAXC software, version 2.4). The cysteine accessibility experiments required the incubation of 2-amino-ethyl-methanesulphonate (MTSEA), prepared in Krebs-Ringer solution immediately before application, with HEK cells for 1 min at a concentration of 3 mM (Insight Biotechnology, Ltd).

Electrophysiology—An Axopatch 200B amplifier (Axon Instruments) recorded whole-cell currents from single HEK cells using the patch clamp technique. HEK cells exhibited resting potentials between −10 and −40 mV and were voltage-clamped at a −40 mV holding potential. The cells were visualized with differential interference contrast optics using a Nikon Optiphot microscope with an epifluorescence attachment to identify green fluorescent protein-transfected cells. A Y-tube was used to rapidly apply drugs and Krebs solutions (exchange rate ~50–100 ms) to the recorded cells. Patch electrodes were fabricated using a Narashige PC-10 puller with resistances, after polishing, of 4–5 megohms. All recordings were performed in constantly perfusing Krebs-Ringer solution at room temperature (20–22 °C).

Data Acquisition and Analysis—Recorded currents were filtered using a high pass Bessel filter at 3 kHz (−36 db/octave), and series resistance compensation was achieved up to 70%. Data were recorded in 20-s acquisition epochs directly to a Pentium IV, 1.8 GHz computer into Clampex software, version 8.0, via a Digidata 1322A (Axon Instruments) sampling at 200-μs intervals. Zn^{2+} was co-applied with the agonist to attenuate any delayed onset of Zn^{2+}-mediated inhibition. Strychnine and picrotoxin were pre-incubated for 15 s, sufficient to attain equilibrium, and then also co-applied with the agonist. The digitized membrane current records were analyzed off-line using Axoscope, version 8.2. Biphasic (potentiation and inhibition) Zn^{2+} concentration response curves were fitted according to a modified Hill equation as previously described (26). Where a single component to the concentration response relationships was evident, it was fitted with a form of the Hill equation. For the agonist and Zn^{2+} concentration potentiation curves, $I = I_{min} + (I_{max} - I_{min})([1/(1 + (EC_{50}/A)^{nH})])$, and for the strychnine and Zn^{2+} concentration-inhibition curves, $I/I_{max} = 1 - [1/(1 + (IC_{50}/B)^{mH})]$.

The EC_{50} represents either the concentration of agonist-inducing or Zn^{2+}-potentiating (A) 50% of the maximal current (I_{max}) evoked or potentiated by a saturating concentration of agonist or Zn^{2+}, and n is the Hill coefficient. For Zn^{2+} potentiation, I_{min} represents the control glycine current in the absence of Zn^{2+} and was set to 100%. For inhibition, the IC_{50} defines the antagonist concentration (B) producing a 50% inhibition of the current, and m_H represents the Hill coefficient. When Zn^{2+} induced a biphasic inhibition, the concentration response data were fitted with a two-component inhibitory curve using $I/I_{max} = 1 - (aB^{mH}/(B^{mH} + IC_{50}{}^{mH})) + (bB^{mH}/(B^{mH} + IC_{50}{}^{mH}))$, where a and b represent the relative proportions of each inhibitory component. All statistical comparisons used an unpaired t test.

Structural Homology Modeling—The mature N-terminal extracellular domain of the hGlyR α_1 subunit was modeled on the crystal structure of the acetylcholine-binding protein (27) using SwissProt DeepView, version 3.7, in accordance with a ClustalW protein alignment. All three-dimensional images were subsequently rendered using the freeware program POV-Ray.

RESULTS

GlyR α_1 and α_2 Exhibit Distinct Sensitivities to Zn^{2+} Potentiation—The sensitivity of the GlyR α_1 and α_2 subtypes to Zn^{2+} potentiation was assessed from whole-cell recordings of half-maximal (EC_{50}) responses to glycine obtained from transfected HEK cells maintained at −40 mV

TABLE ONE

Dose response data for glycine and taurine activation and Zn^{2+} modulation of wild-type and mutant GlyRs

Data represent the mean ± S.E. for *n* number of experiments. ND, not determined.

	Glycine			Taurine			Zn^{2+} (on glycine)			
	Max current	EC_{50}	*n*	EC_{50}	I_{max}[a]	*n*	EC_{50}	Max increase[b]	IC_{50}	*n*
	nA	μM		μM	*% Gly*		μM	%	μM	
Zn^{2+} binding residues										
α_1	4.5 ± 0.5	16 ± 2	5	90 ± 10	~100	5	0.8 ± 0.3	39 ± 8	20 ± 5	4
RIα_1	5.9 ± 0.3	25 ± 4	4	130 ± 30	~100	4	0.8 ± 0.2	42 ± 6	>3000	4
RIα_1H109F[c]	5.1 ± 0.2	28 ± 5	3	ND	ND		1.8 ± 0.5	55 ± 4	>10000	6
RIα_1E192A	3.6 ± 0.7	19 ± 4	3	190 ± 60	~100	3	None	None	710 ± 100	7
RIα_1D194A	4.8 ± 0.4	48 ± 4	3	310 ± 70	~100	3	None	None	270 ± 50	3
RIα_1H215A	3.7 ± 0.2	21 ± 3	3	100 ± 30	~100	3	22 ± 4	28 ± 12	1320 ± 210	4
Acidic non-binding residues										
RIα_1D141A	2.9 ± 1.1	46 ± 7	2	240 ± 80	~100	2	0.5 ± 0.2	41 ± 21	>3000	3
RIα_1D148A	<0.04	ND	9	ND	ND		ND	ND	ND	
RIα_1E191A	4.8 ± 0.6	22 ± 5	3	190 ± 40	~100	3	0.8 ± 0.4	80 ± 50	>3000	3
Residues around Zn^{2+} binding site										
RIα_1K190A	4.5 ± 0.3	9 ± 2	3	80 ± 20	~100	3	0.9 ± 0.7	29 ± 6	ND	3
RIα_1R196A	5.0 ± 0.5	27 ± 6	4	150 ± 50	~100	4	0.6 ± 0.1	34 ± 7	ND	4
RIα_1R213A	5.3 ± 0.2	9 ± 7	3	60 ± 10	~100	3	0.5 ± 0.3	58 ± 30	ND	3
RIα_1E217A	4.2 ± 0.8	21 ± 5	3	120 ± 50	~100	3	0.9 ± 0.3	37 ± 3	ND	4

[a] The maximal inducible current by taurine as a percentage of the maximal glycine-evoked current in the same cell.
[b] The maximum percentage potentiation by Zn^{2+} of a 50% maximal (EC_{50}) agonist-induced response.
[c] This mutation did cause some disruption to other receptor properties, such as a decrease in the rate of activation (unpublished observations). For this reason it was not used as a general background mutant, in preference to H107N, to disrupt inhibition in this study.

holding potential (Fig. 1*A*). To accurately compare the modulation of GlyR α_1 and GlyR α_2 at submicromolar concentrations of Zn^{2+}, the buffer tricine (25) was used to remove Zn^{2+} contamination in the external Krebs solution (22). The α_1 subtype, considered to be an adult form of the GlyR and highly expressed throughout the spinal cord and brainstem (1), exhibited a very high sensitivity to Zn^{2+} potentiation with an EC_{50} of only 37 ± 10 nM ($n = 5$) (Fig. 1*B*). This sensitivity is comparable with the high affinity inhibitory Zn^{2+} site found on the *N*-methyl-D-aspartate receptor NR2A subunit (25). By comparison, the principal embryonic subtype GlyR α2 (1) also displayed a high nanomolar sensitivity to Zn^{2+} potentiation with an EC_{50} of 540 ± 180 nM ($n = 5$) but was nevertheless 15-fold less sensitive than the GlyR α_1 isoform ($p < 0.05$). This difference in sensitivity was unaffected by co-expression with the GlyR ancillary β subunit ($p < 0.05$) (Fig. 1*C*), which assemble to form αβ heteromeric receptors, as confirmed by an approximate 20-fold shift in the sensitivity to picrotoxin (data not shown) (28). The Hill slopes for Zn^{2+}-mediated potentiation varied between 1.2 and 1.5, suggesting more than one Zn^{2+} ion was probably coordinated by each receptor. To identify the structural determinant(s) responsible for differential Zn^{2+} sensitivity, the extracellular domains were scanned for the classical Zn^{2+} binding residues, Cys, Asp, Glu, and His (9), focusing particularly on differences between GlyR α_1 and α_2. On this basis, four residues were prioritized (Fig. 1*D*). Upon individual substitution of the GlyR α_1 variants into GlyR α_2, no influence on Zn^{2+} sensitivity was observed for S179E, D180Q, or E187D mutated receptors (data not shown). However, a single conservative E201D substitution was found to be sufficient and necessary to enable GlyR α_2 to exhibit a similar sensitivity to GlyR α_1 toward potentiation by Zn^{2+} (Fig. 1, *B* and *D*).

A Cluster of GlyR α_1 Residues Are Essential for Zn^{2+} Potentiation—The discovery that GlyR α_1 Asp-194 (which corresponds to GlyR α_2 Glu-201) is capable of influencing the sensitivity to potentiating Zn^{2+}, suggested that this moiety might be a direct contributor to Zn^{2+} binding, forming part of the potentiation site. This hypothesis was examined by mutating α_1 Asp-194 to alanine, a residue incapable of coordinating Zn^{2+}. However, because of the biphasic nature of Zn^{2+} action at the GlyR, where Zn^{2+} potentiates at nanomolar to low micromolar concentrations and inhibits at doses >10 μM (8), any attempt to measure a reduced sensitivity to Zn^{2+} potentiation might be occluded by the onset of Zn^{2+} mediated inhibition. To obviate this problem, all experiments to identify the Zn^{2+} potentiation binding site were performed using an H107N "background" mutation (hereafter referred to as "reduced inhibition" (RI)). This mutation dramatically attenuated the GlyR sensitivity to Zn^{2+} inhibition, increasing the Zn^{2+} IC_{50} from 15 μM to >3 mM without affecting other macroscopic properties of the receptor, particularly the sensitivity of the receptor to Zn^{2+} potentiation (see below next paragraph and TABLE ONE).

To investigate the high potency Zn^{2+} potentiation phenomenon on the background of a low sensitivity Zn^{2+} inhibition component, it was necessary to fully characterize the modulatory curves over a wide concentration range from 0.01 μM to 3 mM. As tricine can only effectively buffer Zn^{2+} concentrations below 1 μM, it was not included in these comparisons. In accord with previous studies (10, 22), the apparent sensitivities to potentiating Zn^{2+} of the wild-type receptor and RIα_1 were lower in the absence of tricine because of the competing background Zn^{2+} present in the external solution, although the relative EC_{50} values remained indistinguishable between the two receptors, (Zn^{2+} EC_{50} values: α_1 wild-type, 0.8 ± 0.3 μM; RIα_1, 0.8 ± 0.2 μM; $n = 4$; $p > 0.05$) (TABLE ONE).

To assess the significance of prospective binding site residues for Zn^{2+} potentiation, the consequences of their replacement were compared for two GlyR agonists, glycine and taurine. This is necessary, as previously identified residues, which have been postulated to be part of a potentiating Zn^{2+} binding site, ablated enhancement of responses to one agonist but not the other presumably due to indirect affects on downstream transduction mechanisms (12). This emphasized the potential importance of Asp-194, because the Zn^{2+} potentiation of both

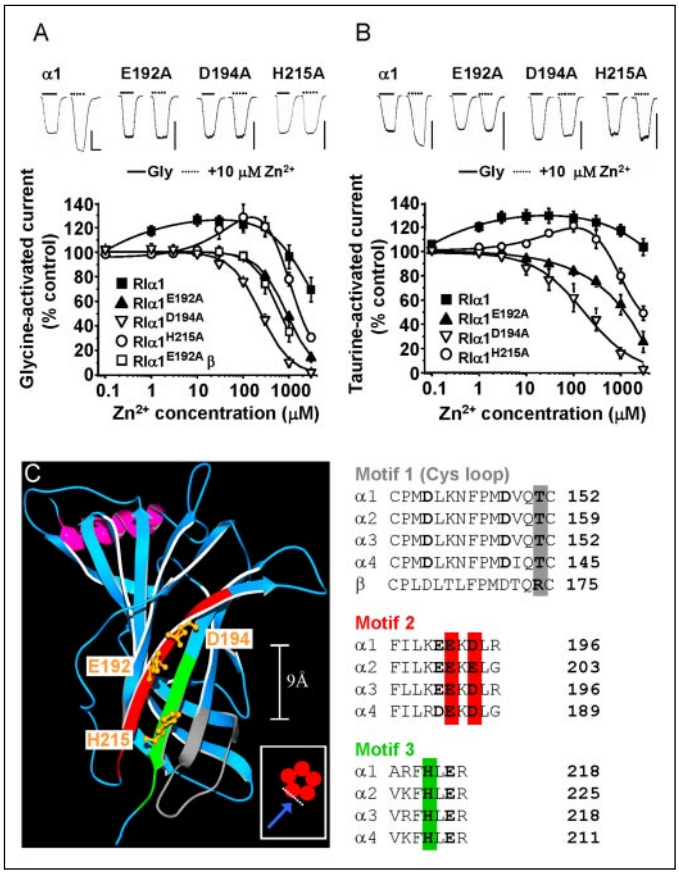

FIGURE 2. **GlyR α_1 subunit residues that affect Zn^{2+} potentiation.** Zn^{2+} concentration response curves for the modulation of EC_{50} responses to glycine (*A*) and taurine (*B*) constructed for mutant homomeric GlyRs $RI\alpha_1$, $RI\alpha_1$E192A, $RI\alpha_1$D194A, and $RI\alpha_1$H215A and one heteromeric GlyR, $RI\alpha_1$E192Aβ. All experiments were performed on a background mutant receptor, GlyR α_1H107N, that exhibited a reduced inhibition (*RI*) to Zn^{2+}. Note the absence of any Zn^{2+} potentiation for most of the mutant receptors, apart from $RI\alpha_1$ and $RI\alpha_1$H215A. The *insets* show typical glycine and taurine (EC_{50})-activated currents in the absence (*continuous line*) and presence of 10 μM Zn^{2+} (*dotted line*). *C*, color-coded amino acid motifs identified in the N-terminal domain of the GlyR α_1 subunit and homologous GlyR α and β subunits that reside in close proximity to the previously identified α_1D194A. The single extracellular domain in the GlyR structural model illustrates the side chains of three putative Zn^{2+} binding residues. The α-helical section at the start of the mature protein is shown in *pink*. The *inset* is a plan view of the GlyR pentamer (*red circles* represent the extracellular subunit N-terminal domains), and the *arrow* denotes the viewing angle. The protein alignments show potential Zn^{2+} binding residues in *bold* in each motif, whereas important residues for Zn^{2+} potentiation are on color-coded backgrounds. A divergent $\alpha\beta$ residue in the Cys loop is also *highlighted* in *gray*.

glycine- and taurine-activated (EC_{50}) responses was ablated in the $RI\alpha_1$D194A receptor (Fig. 2, *A* and *B*). As expected, removing Zn^{2+} potentiation led to an apparent increase in sensitivity to Zn^{2+} inhibition, with the IC_{50} shifting from >3000 to 270 ± 50 μM ($n = 3$). This is probably a consequence of Zn^{2+} potentiation and inhibition having overlapping concentration ranges; therefore, by removing potentiation, the inhibitory component appears to have a lower threshold. We cannot discount the possibility that there is some allosteric interaction between the two Zn^{2+} sites, but this would seem unlikely, as disruption of the inhibitory site does not affect Zn^{2+} potentiation (29). Furthermore, although not a guarantee of independence, Asp-194 of the putative potentiation site is predicted to reside on the external face of the GlyR N terminus (Fig. 2*C*), far away from the inhibitory Zn^{2+} site located on the opposite face of the subunit (30).

To elucidate which residues were capable of interacting with GlyR α_1 Asp-194 in forming the putative Zn^{2+} potentiation binding site, classical Zn^{2+} binding residues were selected from motifs predicted to lie structurally close to Asp-194, according to a GlyR homology model based on the acetylcholine-binding protein (Fig. 2*C*). The selected residues Asp, Cys, Glu, His, and also a Thr (threonine residues have been previously implicated in Zn^{2+} inhibition of GlyRs) (10, 29) were sequentially substituted with alanine. This strategy identified Glu-192 and His-215 as potential contributors to the Zn^{2+} potentiation site (Fig. 2*C*). The mutated GlyR $RI\alpha_1$E192A was unresponsive to Zn^{2+} potentiation, whereas $RI\alpha_1$H215A exhibited a markedly reduced sensitivity to Zn^{2+} potentiation by ~30-fold (Fig. 2, *A* and *B*). The EC_{50} for Zn^{2+} potentiation of glycine responses was increased from 0.8 ± 0.2 μM for $RI\alpha_1$ to 22 ± 4 μM for $RI\alpha_1$H215A ($n = 4$; $p < 0.05$). This reduction in Zn^{2+} sensitivity was directly comparable with that observed when the GlyR was activated by taurine (EC_{50}, 0.9 ± 0.3 to 21 ± 4 μM, respectively; $n = 4$; $p < 0.05$). As previously, removing or reducing Zn^{2+} potentiation increased the apparent sensitivity to Zn^{2+} inhibition for both of these mutants. Moreover, substituting other acidic candidate residues for alanines (highlighted in Fig. 2*C*) had no effect on the potency of Zn^{2+} potentiation. For all three RI mutants α_1E192A, α_1D194A, and α_1H215A, the maximal responses evoked by the agonists glycine and taurine were indistinguishable from the wild-type receptor, and only $RI\alpha_1$D194A exerted a modest 3-fold increase in the agonist EC_{50} values (TABLE ONE), suggesting that these mutations selectively affected the Zn^{2+} potentiation binding site and did not exert a general perturbation on GlyR function. Most importantly, the GlyR homology model (Fig. 2*C*) predicts that Glu-192, Asp-194, and His-215 reside in close proximity to one another on the outside face of the N-terminal extracellular domain. Typically, functional groups involved in direct coordination of Zn^{2+} lie within 2–5 Å of the divalent ion (9), which is easily accommodated by the predicted distances between the three residues identified on the GlyR model (Fig. 2*C*). To highlight the localized specific role this domain plays in Zn^{2+} potentiation, scanning alanine mutagenesis was performed on other residues that lie immediately to either side of the putative Zn^{2+} binding site and that are also predicted to have externally orientated side chains. These mutated GlyRs (RI mutants α_1K190A, α_1R196A, α_1R213A, and α_1E217A) did not affect the glycine, taurine, or Zn^{2+} EC_{50} values, the maximal Zn^{2+} potentiation, or the maximal glycine-activated current (supplemental Fig. 1). In addition, co-expression of a GlyR $RI\alpha_1$E192A with the β subunit did not recover Zn^{2+}-mediated potentiation, suggesting the β subunit is unable to compensate or provide a Zn^{2+} potentiation site of its own ($n = 3$) (Fig. 2*A*).

Asymmetry of Function at the Putative Zn^{2+} Potentiation Binding Site—Demonstrating that this discrete domain is accessible to water is a vital requirement for any dynamic Zn^{2+} binding site and would strengthen the conclusion that the identified residues may act as direct coordinators of Zn^{2+}. We determined this by individual cysteine substitutions of GlyR α_1 Glu-192, Asp-194, and His-215, which were then exposed to the cysteine-modifying reagent MTSEA. If MTSEA covalently binds to the potentiation site, it will replace a Zn^{2+}-coordinating Cys moiety with a positively charged amine group, which should attenuate the Zn^{2+} potentiation of glycine-activated currents. Pre-application of 3 mM MTSEA for 1 min to the control GlyR $RI\alpha_1$ did not affect Zn^{2+} potentiation (Fig. 3*A*) or the glycine EC_{50} and glycine maximal responses (data not shown). Upon individual replacement of Glu-192, Asp-194, and His-215 with cysteine, GlyRs were generated that retained high sensitivities to Zn^{2+} potentiation, with EC_{50} values for Zn^{2+} within 10-fold of the wild-type receptor ($n = 4$) (Fig. 3, *B–D*). This was not surprising, as cysteine is quite capable of coordinating Zn^{2+}. However, following exposure to MTSEA, $RI\alpha_1$D194C and $RI\alpha_1$H215C were rendered unresponsive to Zn^{2+} potentiation, suggesting that the side chains of both of these residues are surface-exposed and important for Zn^{2+} potentiation. The sensitivity of $RI\alpha_1$E192C, however, was largely unaffected

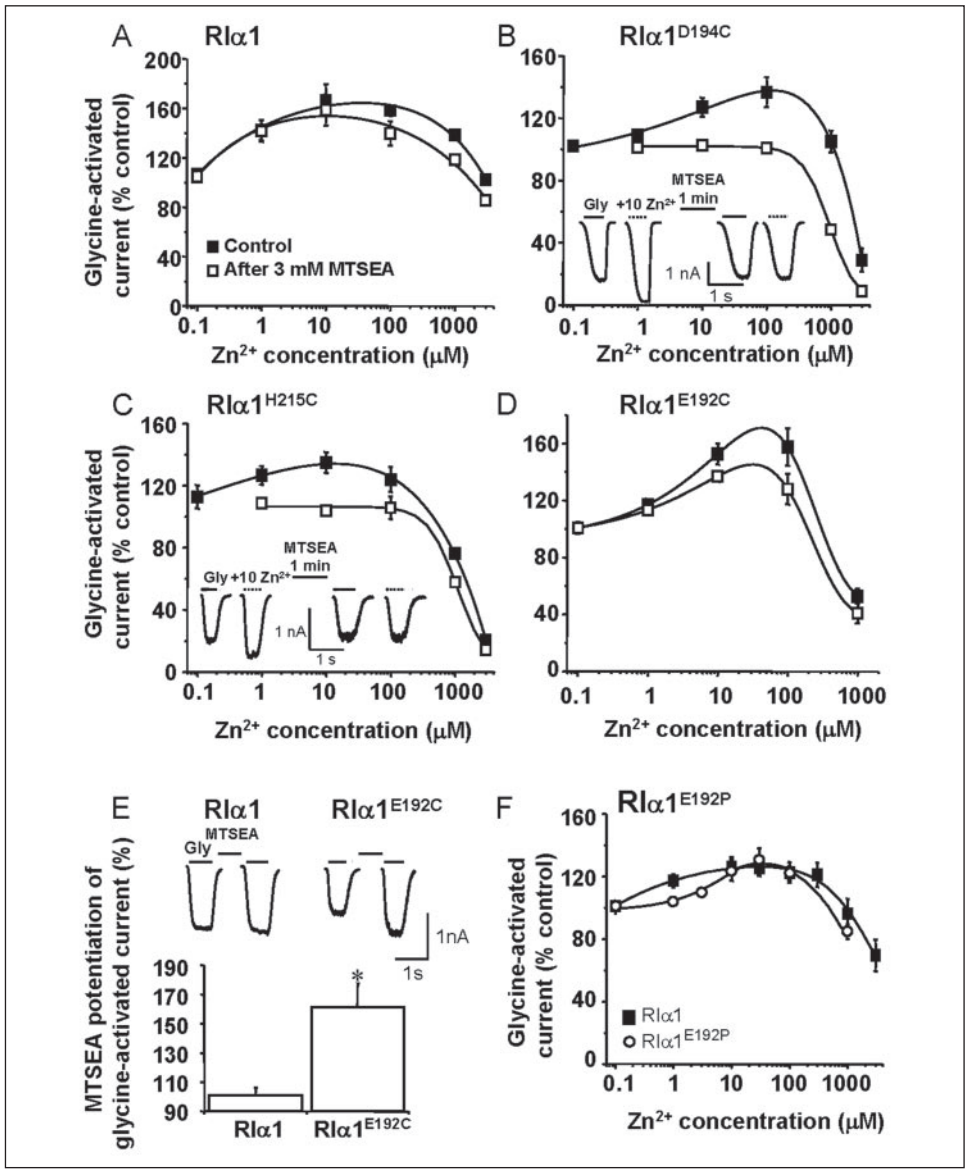

FIGURE 3. **Covalent modification by MTSEA affects Zn^{2+} potentiation of Gly α_1 receptors.** Shown are Zn^{2+} concentration response curves for the modulation of EC_{50} glycine responses measured before and after exposure to 3 mM MTSEA for 1 min for the receptors RIα_1 (*A*) and for those receptors mutated to incorporate cysteines at putative Zn^{2+} binding residues RIα_1^{D194C} (*B*), RIα_1^{H215C} (*C*), and RIα_1E192C (*D*) ($n = 4$). The *insets* present example glycine (EC_{50})-activated currents in the absence (*solid line*) and presence (*broken line*) of 10 μM Zn^{2+} before and after 3 mM MTSEA. *E*, glycine (EC_{50}) current amplitudes for RIα_1 and RIα_1E192C before and after 3 mM MTSEA. The *inset* depicts typical glycine-activated currents for the same concentration of glycine before and after exposure to MTSEA. *F*, Zn^{2+} concentration response curves for the modulation of EC_{50} glycine responses on RIα_1 and RIα_1E192P to explore whether inducing specific conformational restraints on the peptide backbone at this location affects Zn^{2+} potentiation ($n = 4$). * denotes significance at $p < 0.05$

($n = 4$) (Fig. 3, *B–D*). The binding of MTSEA alone was insufficient to induce potentiation of glycine-activated responses at RIα_1D194C or RIα_1H215C (Fig. 3, *B* and *C*). Surprisingly, MTSEA did increase glycine potency in the absence of Zn^{2+} for RIα_1E192C, potentiating the glycine response by 61 ± 16% ($n = 4$, $p < 0.05$) (Fig. 3*E*). Thus, Glu-192 appears to be accessible to MTSEA, although this covalent modification did not affect the ability of Zn^{2+} to bind to the receptor. If the carboxyl side chain of Glu-192 was not directly coordinating Zn^{2+}, then perhaps substitution of this residue with alanine would perturb the β-strand backbone, which then would either indirectly disrupt the Zn^{2+} potentiation site or disrupt a possible contribution of the polar peptide backbone at this locus for Zn^{2+} coordination. To determine the relevance of the backbone at Glu-192, this residue was mutated to proline (RIα_1E192P), an amino acid associated with placing conformational restraints upon peptide backbones (31). Even though proline cannot coordinate Zn^{2+}, potentiation in this mutated receptor was retained, although at a 5-fold reduced sensitivity (0.8 ± 0.2 μM for RIα_1 and 4.2 ± 0.8 μM for RIα_1E192P ($n = 4$, $p < 0.05$) (Fig. 3*F*). This suggested that, to retain Zn^{2+}-mediated potentiation, this region must retain a specific conformation of the backbone at Glu-192, which can be accommodated by the introduction of a proline but not by insertion of an alanine. Of course, without precise structural data, it is not possible to infer any specific details about the structural organization at this locus other than that the backbone is particularly sensitive to perturbation in a fashion that affects Zn^{2+} potentiation. As a control for this strategy, the mutant GlyR RIα_1D194P ablated Zn^{2+}-mediated potentiation, an outcome that is expected if, indeed, the side chain moiety is contributing to Zn^{2+} coordination at this particular position (data not shown).

Although the current data most strongly support a role for GlyR α_1 Asp-194 and His-215 in direct Zn^{2+} coordination, the GlyR RIα_1H215A substitution attenuated the sensitivity to Zn^{2+}, whereas GlyR RIα_1D194A entirely removed Zn^{2+} potentiation (Fig. 2, *A* and *B*). To examine the actual extent by which Zn^{2+}-mediated potentiation was affected by perturbation of Asp-194, it was necessary to further disrupt the competing inhibitory Zn^{2+} site such that inhibition does not occlude any remaining sensitivity to Zn^{2+} potentiation. A number of GlyRs were generated to ablate Zn^{2+}-mediated inhibition based on previously identified targets (10, 26, 29). Of these, the one that most effectively attenuated Zn^{2+}-mediated inhibition while still retaining mostly "normal" receptor function in terms of agonist specificity, sensitivity,

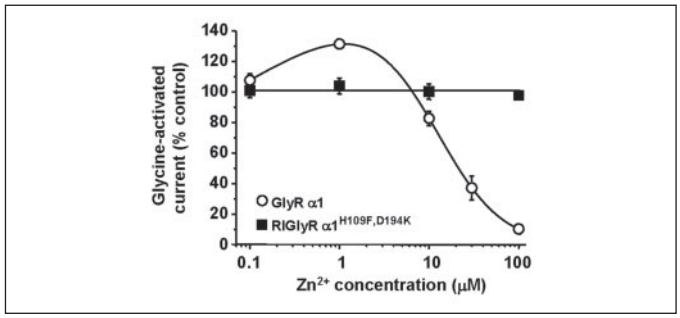

FIGURE 4. **Ablation of Zn^{2+} inhibition and potentiation in GlyR α_1.** Zn^{2+} concentration response curves for the modulation of EC_{50} glycine responses on the wild-type GlyR α_1 and the triple mutant receptor RIα_1H109F,D194K. This mutant lacks two vital elements of the GlyR inhibitory Zn^{2+} site (His-107 replaced with Asn, denoted as reduced inhibition (*RI*), and His-109). Note that the mutation of Asp-194 is sufficient to remove enhancement up to 100 μM Zn^{2+}, demonstrating its crucial requirement for Zn^{2+} potentiation.

and maximal activation was the RIα_1H109F receptor (TABLE ONE). On this new mutant background, we introduced the mutation D194K to prevent any Zn^{2+} binding by replacing aspartate with a positively charged amine group. The resultant GlyR RIα_1H109F,D194K was unaffected by 0.1–100 μM Zn^{2+} ($n = 4$), a concentration range over which the wild-type GlyR α_1 underwent its full Zn^{2+} modulatory profile. This demonstrated that the potentiating Zn^{2+} site was effectively ablated up to 100 μM Zn^{2+}, a concentration that is 125-fold greater than the Zn^{2+} EC_{50} value of 0.8 ± 0.3 μM on the wild-type GlyR α_1 (Fig. 4).

GlyR α_1 Thr-151 Is a Critical Control Element for Zn^{2+} Potentiation—Besides the classical Zn^{2+} binding moieties of the potentiating site, we also identified a nearby polar residue at position 151 located in the Cys loop called *L7* (27). Alanine substitution of threonine 151 generated an RIα_1T151A GlyR that was insensitive to the potentiating effect of Zn^{2+} (Fig. 5, *A* and *D*). Although the lack of potentiation was clear, there was also an unusual additional effect revealed in the form of a novel biphasic sensitivity to Zn^{2+} inhibition, with high (IC_{50} = 1.6 ± 0.6 μM, $n = 5$) and low potency components (IC_{50} = 1040 ± 290 μM, $n = 5$). This biphasic inhibitory profile was also apparent when taurine was the agonist (IC_{50} = 3.2 ± 0.8 μM and 2840 ± 820 μM, $n = 5$) (Fig. 5*B*). Intriguingly, the IC_{50} value for the high sensitivity inhibitory component is directly comparable with the original Zn^{2+} EC_{50} value of 0.8 ± 0.2 μM for potentiation at RIα_1. Conceivably, the α_1 T151A substitution may have converted the Zn^{2+} potentiation site to a high sensitivity Zn^{2+} inhibitory site. In support of this hypothesis, incorporating the mutation E192A (producing GlyR RIα_1T151A,E192A), designed to disrupt the Zn^{2+} potentiating site, mostly removed the high potency inhibitory component (Fig. 5*A* and TABLE TWO). Furthermore, the lower potency component was attributed to the previously identified Zn^{2+} inhibitory site (26), because restoration of this site by reinstating His-107 (producing GlyR α_1T151A) increased the relative sensitivity to inhibition (Fig. 5, *A* and *B*). The effects of similar experiments, introducing D194A or H215A onto the RIα_1T151A-mutated GlyR, were not possible, as these receptors (RIα_1T151A,D194A, $n = 24$; and RIα_1T151A,H215A, $n = 16$) were effectively non-functional with very low maximal currents (TABLE TWO).

To further characterize the role of Thr-151, this residue was mutated to two variants selected from the Cys loop receptor family, including an arginine from the GlyR β subunit, which previously appeared incapable of supporting Zn^{2+} potentiation, and an Asn from the serotonin type 3A receptor, which displays a comparable sensitivity profile to the GlyR α subunit with regard to Zn^{2+} potentiation (32, 33). These mutated GlyRs, RIα_1T151R and RIα_1T151N, failed to support Zn^{2+} potentiation

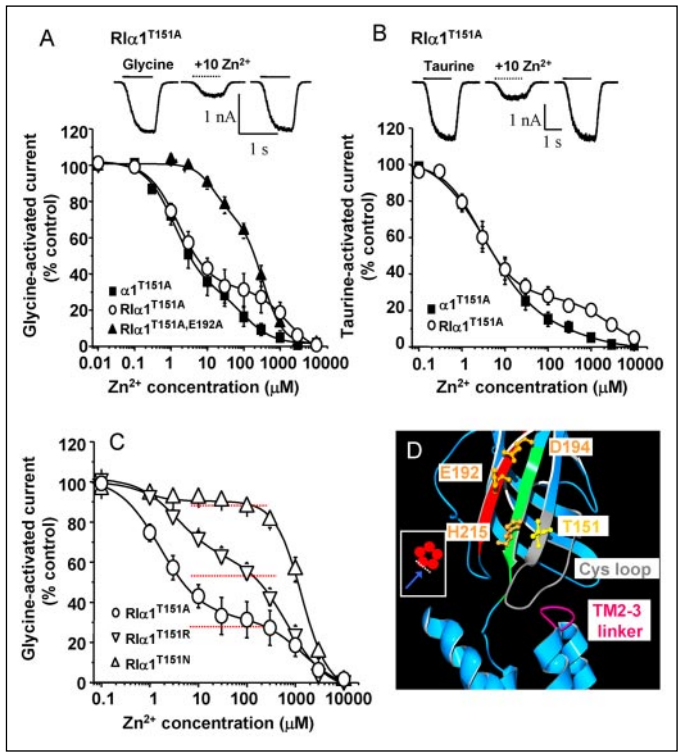

FIGURE 5. **Role of Thr-151 in signal transduction from the Zn^{2+} potentiation site.** Zn^{2+} concentration response curves for the modulation of glycine (*A*)- and taurine (*B*)-activated currents (at their EC_{50} values) for mutant GlyR α_1 homomers. Note that potentiation is abolished by mutation of Thr-151 and replaced with a novel biphasic inhibition. The sensitivity of the high potency component is dependent on Glu-192, a residue originally involved in Zn^{2+} potentiation, whereas the low potency component is dependent on His-107, a residue involved in Zn^{2+} binding to the discrete inhibitory Zn^{2+} site. The *insets* show typical EC_{50} glycine and taurine currents in the absence (*continuous line*) and presence (*dotted line*) of 10 μM Zn^{2+}. *C*, sequential mutation of Thr-151 affects the contribution of the high potency component to the Zn^{2+} concentration inhibition curve, denoted by the *broken lines* ($n = 4–6$). *D*, a single GlyR α_1 subunit N-terminal extracellular domain, highlighting Thr-151 (*yellow*) within the putative Cys loop-gating domain (*gray*) (other colored motifs and residues are the same as in Fig. 2), and its proximity to another important determinant in gating, the TM2-TM3 linker region (*maroon*), which rests above the transmembrane helices that form the receptor ion channel (*shaded blue*). The *inset* depicts the viewing angle (*blue arrow*) of the GlyR pentamer.

and instead revealed biphasic inhibitory profiles for glycine-activated responses (Fig. 5*C*). The sensitivity of the high potency inhibitory component was comparable with that seen for RIα_1T151A (RIα_1T151R IC_{50} = 3.6 ± 0.7 μM and RIα_1T151N IC_{50} = 1.6 ± 0.7 μM; $n = 4$; $p > 0.05$). However, the maximal contribution of the high potency inhibitory component was reduced to 39 ± 3% for RIα_1T151R and to just 6.5 ± 0.3% for RIα_1T151N from 73 ± 8% for RIα_1T151A (Fig. 5*C*), suggesting the nature of the residue at position 151 was important in determining both the direction and the extent of the Zn^{2+} effect.

GlyR α_1 Thr-151 Influences Apparent Agonist Gating—As Thr-151 resides in the Cys loop, a domain that is important for agonist gating in this receptor superfamily (34), each of these mutations was assessed for their effect on agonist potencies. All of the mutations α_1T151A, RIα_1T151A, RIα_1T151R, RIα_1T151A,E192A, and RIα_1T151N caused a progressive reduction in sensitivity to both glycine and taurine with RIα_1T151N demonstrating 11- and 23-fold increases in the EC_{50} values for glycine and taurine, respectively ($n = 5$; $p < 0.05$) (Fig. 6, *A* and *B*; TABLE TWO). In accord with the possibility of Thr-151 being involved in ion channel gating, the percentage of maximum current evoked by the lower potency agonist taurine compared with maximal glycine responses in the same cell decreased significantly from 100% and 98 ± 2% in RIα_1 and RIα_1T151A, respectively, to 90 ± 3% for RIα_1T151R, 65 ± 4.3% for RIα_1T151A,E192A and 46 ± 6% for

TABLE TWO

Dose response data for glycine and taurine activation and Zn^{2+} modulation on Thr151 mutated α_1 GlyRs

Data represent the mean ± S.E. for *n* number of experiments. ND, not determined.

	Glycine			Taurine			Zn^{2+} (on glycine)			
	Max current	EC_{50}	*n*	EC_{50}	I_{max} [a]	*n*	Zn^{2+} $IC_{50}A$ [b]	$IC_{50}A$ Max [c] inhibition	Zn^{2+} $IC_{50}B$ [d]	*n*
	nA	*μM*		*μM*	*% Gly*		*μM*	*%*	*μM*	
Agonist and Zn^{2+} transduction Thr151 residue mutations										
α_1T151A	4.7 ± 0.6	53 ± 9	4	330 ± 60	~100	4	2.9 ± 2.0	68 ± 7	160 ± 60	4
RIα_1T151A	4.0 ± 0.4	63 ± 12	5	380 ± 80	97 ± 4	4	1.6 ± 0.6	73 ± 8	1040 ± 290	5
RIα_1T151N	2.9 ± 0.5	180 ± 30	7	2060 ± 230	46 ± 6	5	1.6 ± 0.7	7 ± 0.4	1410 ± 210	4
RIα_1T151R	3.8 ± 0.9	95 ± 7	3	560 ± 130	93 ± 3	4	3.6 ± 0.4	39 ± 3	710 ± 130	4
T151 combined with residues within and around the Zn^{2+} binding site										
RIα_1T151A, E192A	1.9 ± 0.5	170 ± 10	7	960 ± 160	65 ± 4	7	16 ± 3	32 ± 4	390 ± 60	3
RIα_1T151A, D194A	0.15 ± 0.1	220 ± 20	24	ND	33 ± 6	20	ND	ND	ND	ND
RIα_1T151A, H215A	0.1 ± 0.04	380 ± 30	16	ND	40 ± 10	15	ND	ND	ND	ND

[a] The maximal current induced by taurine as a percentage of the maximal glycine-evoked current in the same cell.
[b] High potency Zn^{2+} IC_{50}.
[c] Percentage reduction achieved by high potency concentrations of Zn^{2+} of 50% maximal glycine-activated currents.
[d] Low potency Zn^{2+} IC_{50}.

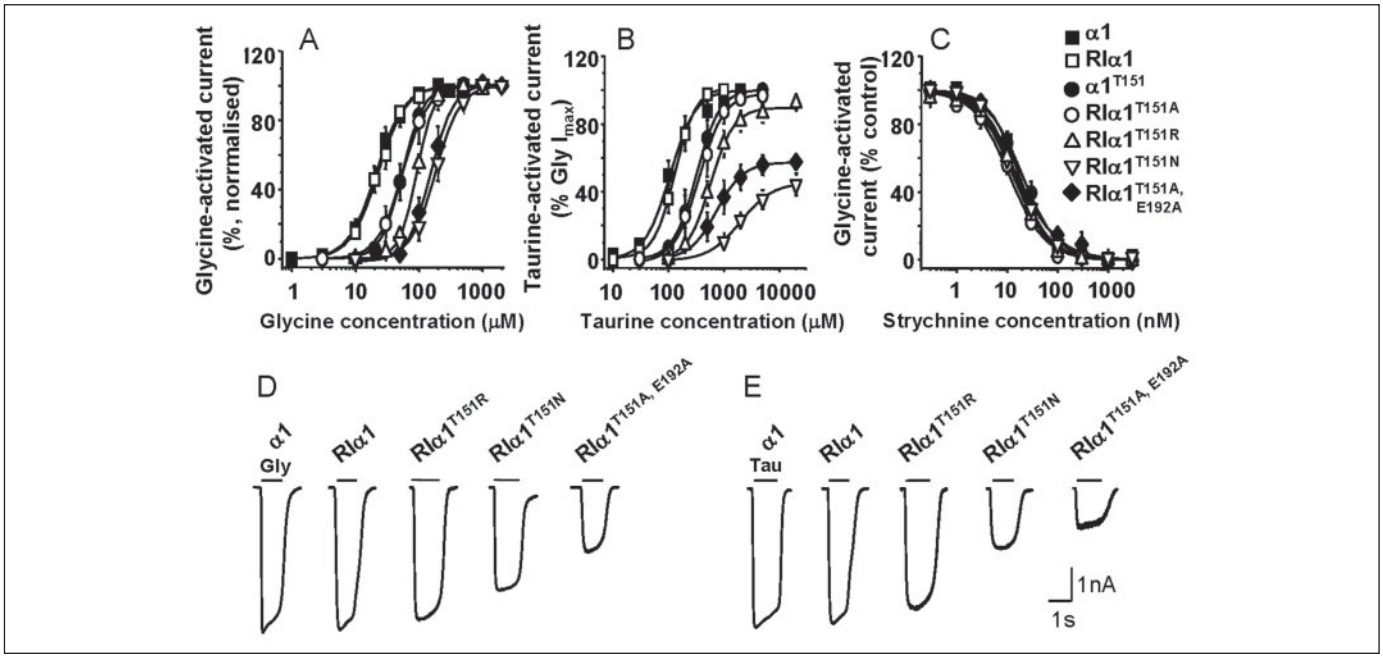

FIGURE 6. **Substitution at T151 disrupts agonist sensitivity of the GlyR.** Glycine (*A*), and taurine (*B*) concentration response curves for a series of α_1 Thr-151 mutants ($n = 4–11$). The glycine and taurine curves are normalized in each cell to the maximum response to glycine (2 mM). Note the decrease in the relative efficacy for taurine evident from the reduced maximal responses. *C*, strychnine concentration inhibition curves were determined for the antagonism of EC_{50} glycine-activated currents for the same series of receptors. The lack of deviation between the curves suggests the agonist binding region is not distorted by the mutations, supporting the hypothesis that disruption impinges on receptor gating not ligand binding. *D* and *E*, display of representative maximal glycine- and taurine-activated currents, respectively, recorded from HEK cells expressing the Thr-151 mutants.

RIα_1T151N ($n = 4–7$; $p < 0.05$) (Fig. 6, *B* and *E*; TABLE TWO). In addition, the maximum glycine-evoked currents were also significantly reduced from 4.5 ± 0.4 nA for wild-type GlyR α_1 to 1.9 ± 0.5 nA for RIα_1T151A,E192A and to 2.9 ± 0.5 nA for RIα_1T151N ($n = 5–12$, $p < 0.05$) (Fig. 6*D*). These mutated receptors did not substantially distort the region of agonist binding, as sensitivities to the competitive antagonist strychnine were directly comparable with the wild-type GlyR (Fig. 6*C*). The non-functional nature of the receptors RIα_1T151A,D194A and RIα_1T151A,H215A precluded their study in this experiment (TABLE TWO). Additional mutations at GlyR α_1 Thr-151 to Cys, Asp, Glu, Ser, and Phe revealed no obvious relationship between side chain polarity and the volume requirements of a residue occupying position 151 for receptor activation (supplemental Table 1; supplemental Fig. 2).

DISCUSSION

This study reports the first molecular description of a Zn^{2+} potentiation site on a Cys loop ligand-gated ion channel. The residues Asp-194, His-215, and the peptide backbone located at Glu-192 in GlyR α_1 are all predicted to reside in close structural proximity to one another, and they all influence Zn^{2+} potentiation in accord with a role in binding. Each of these residues is chemically adept at coordinating Zn^{2+}, and when this capacity is annulled, through alanine substitution, the sensitivity to Zn^{2+} was either attenuated (as for RIα_1H215A) or entirely ablated (as for RIα_1E192A and RIα_1D194A). Moreover, experiments using MTSEA demonstrated that the residues in this putative site are accessible to this water-soluble compound and therefore must also be accessible to dynamic Zn^{2+} binding. Additionally, as Zn^{2+} potentiation

of both glycine- and taurine-activated currents was similarly affected by these mutations, it is likely these residues are either part of a universal Zn^{2+} binding site or participate in the process of allosteric signal transduction from such a binding site. Finally, the analysis of the α_1E192P receptor suggested that this location might contribute structurally to the site in a manner dependent upon the restraints of the peptide backbone. If the backbone itself can contribute to Zn^{2+} binding, then the site isolated here requires only a fourth coordinating ligand for completion, and in the case of reversible Zn^{2+} binding catalytic sites, this is predominantly provided by an activated water molecule (9).

In addition to those residues thought to line the Zn^{2+} binding site, Thr-151 was also identified as an important transduction component for this site because of its nearby location. The exact nature of the residue introduced at position 151 did not alter the potency of Zn^{2+}, precluding an involvement in binding, but it was able to determine the "direction of output" from the Zn^{2+} site to be either potentiating (for threonine) or inhibitory (for alanine, arginine, and asparagine). Furthermore, the type of residue at position 151 also controlled the efficacy of inhibition from the Zn^{2+} site. As this site is quite distinct in its structure and location, Thr-151 is most unlikely to be associated with the previously reported Zn^{2+} inhibitory site on GlyR α_1, which resides on the other side of the subunit (10, 26, 30). In accordance with the location of Thr-151 being in the critical Cys loop-gating domain (34–36), this residue was also shown to be an important determinant of agonist potency for receptor activation. Thus, from a molecular perspective, it provides a potential connection between the Zn^{2+} potentiation binding site and the Cys loop-gating domain to possibly increase the efficacy of agonist-induced channel opening. In accordance with Zn^{2+} potentiation being mediated via an increase in agonist efficacy, the partial agonist taurine is converted to a full agonist by Zn^{2+} concentrations that cause potentiation at GlyR α_1 expressed in oocytes (10). Furthermore, residues located in the TM2-TM3 linker, which are predicted to be closely apposed to, and capable of interacting with, the Cys loop-gating domain (27, 37), also affect Zn^{2+}-mediated potentiation (12), as would be expected if there is direct communication between these two domains.

The reversal of signal output, exemplified here by changing Zn^{2+} potentiation to inhibition following the mutation of Thr-151, is not a unique observation for ligand-gated ion channels. Mutation of isoleucine 307 in the TM2 domain of the $GABA_C$ receptor to glutamine reverses the inhibition caused by the neurosteroid 5β-pregnane-3α-ol-20-one on the wild-type receptor to potentiation (38). This suggests that whether a modulator exerts a positive or negative effect on receptor activation may be highly dependent on the nature of the allosteric transduction pathway leading away from the binding site.

CONCLUSIONS

We report here the identification of the Zn^{2+} potentiation binding site on the GlyR and a possible molecular route of action for Zn^{2+} potentiation via the Cys loop channel-gating domain. The Zn^{2+} potentiation site is a novel site on the GlyR clearly distinct from the previously identified interfacial inhibitory Zn^{2+} binding sites for GlyRs (30) and $GABA_A$ receptors (39), which reside on the inside faces of these pentamers. The potentiation site has a high sensitivity to Zn^{2+}, with the EC_{50} estimated at <100 nM, well within the range of current estimates for physiological levels of basal and released Zn^{2+} (40). The location of this site away from the intrasubunit interfaces of the GlyR pentamer may have implications for the manner in which Zn^{2+} achieves its effect, because when Zn^{2+} is bound at the potentiation site, it is predicted to interact with the gating apparatus of the receptor. In contrast, when Zn^{2+} is bound at the interfacial inhibitory site, it acts in an apparent competitive manner, stabilizing the closed agonist-unbound state of the receptor (1).

Acknowledgments—We thank Drs. Alastair Hosie and Philip Thomas for their helpful advice and comments on the manuscript and Dr. Robert Harvey for the wild-type cDNA construct.

REFERENCES

1. Lynch, J. W. (2004) *Physiol. Rev.* **84,** 1051–1095
2. Karlin, A., and Akabas, M. H. (1995) *Neuron* **15,** 1231–1244
3. Pfeiffer, F., Graham, D., and Betz, H. (1982) *J. Biol. Chem.* **257,** 9389–9393
4. Lester, H. A., Dibas, M. I., Dahan, D. S., Leite, J. F., and Dougherty, D. A. (2004) *Trends Neurosci.* **27,** 329–336
5. Harrison, N. L., Kugler, J. L., Jones, M. V., Greenblatt, E. P., and Pritchett, D. B. (1993) *Mol. Pharmacol.* **44,** 628–632
6. Celentano, J. J., Gibbs, T. T., and Farb, D. H. (1988) *Brain Res.* **455,** 377–380
7. Wu, F. S., Chen, S. C., and Tsai, J. J. (1997) *Brain Res.* **750,** 318–320
8. Bloomenthal, A. B., Goldwater, E., Pritchett, D. B., and Harrison, N. L. (1994) *Mol. Pharmacol.* **46,** 1156–1159
9. Auld, D. S. (2001) *Biometals* **14,** 271–313
10. Laube, B., Kuhse, J., and Betz, H. (2000) *J. Physiol.* (*Lond.*) **522,** 215–230
11. Laube, B., Maksay, G., Schemm, R., and Betz, H. (2002) *Trends Pharmacol. Sci.* **23,** 519–527
12. Lynch, J. W., Jacques, P., Pierce, K. D., and Schofield, P. R. (1998) *J. Neurochem.* **71,** 2159–2168
13. Assaf, S. Y., and Chung, S. H. (1984) *Nature* **308,** 734–736
14. Howell, G. A., Welch, M. G., and Frederickson, C. J. (1984) *Nature* **308,** 736–738
15. Xie, X. M., and Smart, T. G. (1991) *Nature* **349,** 521–524
16. Ruiz, A., Walker, M. C., Fabian-Fine, R., and Kullmann, D. M. (2003) *J. Neurophysiol.*
17. Birinyi, A., Parker, D., Antal, M., and Shupliakov, O. (2001) *J. Comp. Neurol.* **433,** 208–221
18. Brown, C. E., and Dyck, R. H. (2002) *J. Neurosci.* **22,** 2617–2625
19. Frederickson, C. J., and Danscher, G. (1990) *Prog. Brain Res.* **83,** 71–84
20. Frederickson, C. J., and Bush, A. I. (2001) *Biometals* **14,** 353–366
21. Smart, T. G., Xie, X., and Krishek, B. J. (1994) *Prog. Neurobiol.* (*Oxf.*) **42,** 393–341
22. Suwa, H., Saint-Amant, L., Triller, A., Drapeau, P., and Legendre, P. (2001) *J. Neurophysiol.* **85,** 912–925
23. Wilkins, M. E., Hosie, A. M., and Smart, T. G. (2002) *J. Neurosci.* **22,** 5328–5333
24. Cubitt, A. B., Heim, R., Adams, S. R., Boyd, A. E., Gross, L. A., and Tsien, R. Y. (1995) *Trends Biochem. Sci.* **20,** 448–455
25. Paoletti, P., Ascher, P., and Neyton, J. (1997) *J. Neurosci.* **17,** 5711–5725
26. Harvey, R. J., Thomas, P., James, C. H., Wilderspin, A., and Smart, T. G. (1999) *J. Physiol.* (*Lond.*) **520,** 53–64
27. Brejc, K., van Dijk, W. J., Klaassen, R. V., Schuurmans, M., van Der, Oost J., Smit, A. B., and Sixma, T. K. (2001) *Nature* **411,** 269–276
28. Pribilla, I., Takagi, T., Langosch, D., Bormann, J., and Betz, H. (1992) *EMBO J.* **11,** 4305–4311
29. Miller, P. S., Beato, M., Harvey, R. J., and Smart, T. G. (2005) *J. Physiol* (*Lond.*) **566,** 657–670
30. Nevin, S. T., Cromer, B. A., Haddrill, J. L., Morton, C. J., Parker, M. W., and Lynch, J. W. (2003) *J. Biol. Chem.* **278,** 28985–28992
31. Yaron, A., and Naider, F. (1993) *Crit. Rev. Biochem. Mol. Biol.* **28,** 31–81
32. Gill, C. H., Peters, J. A., and Lambert, J. J. (1995) *Br. J. Pharmacol.* **114,** 1211–1221
33. Hubbard, P. C., and Lummis, S. C. (2000) *Eur. J. Pharmacol.* **394,** 189–197
34. Kash, T. L., Jenkins, A., Kelley, J. C., Trudell, J. R., and Harrison, N. L. (2003) *Nature* **421,** 272–275
35. Schofield, C. M., Jenkins, A., and Harrison, N. L. (2003) *J. Biol. Chem.* **278,** 34079–34083
36. Schofield, C. M., Trudell, J. R., and Harrison, N. L. (2004) *Biochemistry* **43,** 10058–10063
37. Miyazawa, A., Fujiyoshi, Y., and Unwin, N. (2003) *Nature* **424,** 949–955
38. Morris, K. D., and Amin, J. (2004) *Mol. Pharmacol.* **66,** 56–69
39. Hosie, A. M., Dunne, E. L., Harvey, R. J., and Smart, T. G. (2003) *Nat. Neurosci.* **6,** 362–369
40. Frederickson, C. J., Suh, S. W., Silva, D., Frederickson, C. J., and Thompson, R. B. (2000) *J. Nutr.* **130,** (suppl.) 1471S–1483S